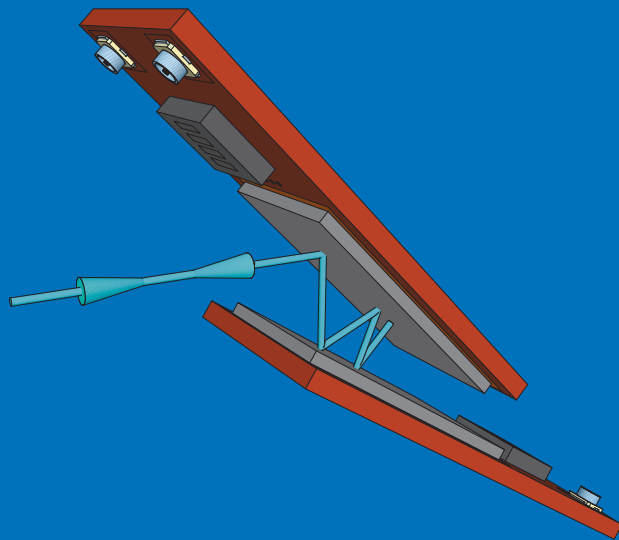# Predictable Quantum Efficient Detector

Meelis-Mait Sildoja

Predictable Quantum Efficient Detector

Meelis-Mait Sildoja

A doctoral dissertation completed for the degree of Doctor of Science (Technology) to be defended, with the permission of the Aalto University School of Electrical Engineering, at a public examination held at the lecture hall S1 of the school on 13 December 2013 at 12.

Aalto University
School of Electrical Engineering
Department of Signal Processing and Acoustics
Metrology Research Institute

Supervising professor
Prof. Erkki Ikonen

Thesis advisor
Dr. Farshid Manoocheri

Preliminary examiners
Prof. Edouard Monakhov, University of Oslo, Norway
Dr. Kathryn Nield, Measurement Standards Laboratory, New Zealand

Opponent
Dr. Marla Dowell, National Institute of Standards and Technology,
USA

NORDIC ECOLABEL

441   697
Printed matter

Abstract

This thesis gives an overview of the Predictable Quantum Efficient Detector designed to measure optical radiation with theoretical relative uncertainty of 1 ppm (parts per million). The device is based on two custom made large area induced junction silicon photodiodes arranged in a wedged trap structure. High internal quantum efficiency (IQE) of the photodiodes is achieved by means of low doping concentration and usage of the reverse bias voltage. The IQE is predicted to be improved furthermore using low operating temperature close to 77 K. The losses due to reflected light are minimized by multiple reflections between the photodiodes. Low losses allow the PQED to work as an ideal quantum detector whose spectral responsivity is determined purely by the fundamental constants h, c, e and vacuum wavelength λ. The remaining minor charge carrier losses are predictable using physical modelling whereas fractional reflectance losses can be measured. These properties classify the PQED as an absolute detector which does not require calibration against any other radiometric primary standard.

The prototype PQED was compared against present primary standard - the cryogenic radiometer – at the wavelengths of 476 nm, 532 nm and 760 nm at room temperature and at liquid nitrogen temperature. Comparisons showed that the predicted external quantum deficiency of the PQED agreed with the measured external quantum deficiency within the expanded uncertainty of 60 ppm to 180 ppm determined by the cryogenic radiometer at both temperatures. These results indicate that the responsivity of the PQED is highly predictable and its uncertainty is comparable with the uncertainty of the conventional cryogenic radiometer. Such data provide evidence that the cryogenic radiometer operated close to 10 K temperatures may be replaced by a PQED operated even at room temperature.

The advantage of the PQED is its simple operation which is comparable with any other silicon based photodetector whereas its optical radiation detection uncertainty is comparable with expensive and sophisticated cryogenic radiometer.

Preface

The research work combined into this thesis has been carried out at the Metrology Research Institute of Aalto University and contains mostly work during the years 2007-2013 within the scope of the European Metrology Research Program project Quantum Candela.

I am most grateful to my supervisor, Professor Erkki Ikonen, for his in-depth guidance, fruitful discussions and for leading me back to trails many times during the evolvement of the work. In similar way I thank my instructor, Dr. Farshid Manoocheri, with whom the exciting scientific collaboration has grown also to good friendship.

I want to thank Dr. Mart Noorma for introducing me the field of optical metrology and Dr. Toomas Kübarsepp for his guidance and being my first supervisor during the Tartu period. From the Institute of Physics of Tartu University I thank Dr. Ants Lõhmus for his help in designing measurement systems which were essential for many of the valuable experimental results.

I thank all my co-authors from several institutions in Finland and abroad. From Metrology Resereach Institute and from MIKES I wish to thank Dr. Mikko Merimaa, Timo Dönsberg and Henrik Mäntynen. My gratitude goes also to Dr. Lutz Werner and Ingmar Müller from PTB and for Dr. Marek Smîd and Geiland Porrovecchio from CMI for their kindness and support during my several visits to Berlin and Prague. The collaborated experiments in these institutions have had an eye opening for me in many ways. The scientific support and contribution of Dr. Jarle Gran form Justervesenet and Dr. Atte Haapalinna from Okmetic Oyj is highly appreciated.

For the warm atmosphere in the Metrology Research Institute I thank all the previous and present people with whom I have had the pleasure to work with, especially Dr. Petri Kärhä, Dr. Saulius Nevas, Dr. Tuomas Hieta, Dr. Maija Ojanen, Dr. Silja Holopainen, Dr. Pasi Manninen, Dr. Markku Vainio, Dr. Ville Ahtee, Dr. Antti Lamminpää, Dr. Jouni Envall, Dr. Mikko Puranen, Dr. Marko Laurila, Dr. Tuomas Poikonen, Priit Jaanson, Aigar Vaigu,

Maksim Shpak, Tomi Pulli, Teemu Kokki, Teemu Koskinen and Hans Baumgartner.

My warm gratitude goes to all my close friends with whom the darker days looked much brighter.

Preliminary examiners Dr. Kathryn Neild and Prof. Edouard Monakhov are thanked for their efforts and encouraging feedback.

I want to thank also CIMO, Aalto University and Academy of Finland for the financial support.

Finally, I thank my parents for their support and patience during my years abroad.

Espoo, November 13, 2013

Meelis-Mait Sildoja

Contents

List of Publications

[I]   M. Sildoja, F. Manoocheri, and E. Ikonen, "Reducing photodiode reflectance by Brewster-angle operation," *Metrologia*, **45**, 11–15, 2008.

[II]   M. Sildoja, F. Manoocheri, and E. Ikonen, "Reflectance calculations for a predictable quantum efficient detector," *Metrologia*, **46**, S151–S154, 2009.

[III]   J. Gran, T. Kübarsepp, M. Sildoja, F. Manoocheri, E. Ikonen, and I. Müller, "Simulations of a predictable quantum efficient detector with PC1D," *Metrologia*, **49**, S130–S134, 2012.

[IV]   M. Sildoja, F. Manoocheri, M. Merimaa, E. Ikonen, I. Müller, L. Werner, J. Gran, T. Kübarsepp, M. Smîd, and M. L. Rastello, "Predictable quantum efficient detector: I. Photodiodes and predicted responsivity," *Metrologia*, **50**, 385–394, 2013.

[V]   I. Müller, U. Johannsen, U. Linke, L. Socaciu-Siebert, M. Smîd, G. Porrovecchio, M. Sildoja, F. Manoocheri, E. Ikonen, J. Gran, T. Kübarsepp, G. Brida, and L. Werner, "Predictable quantum efficient detector: II. Characterization and confirmed responsivity," *Metrologia*, **50**, 395–401, 2013.

[VI]   M. Sildoja, T. Dönsberg, H. Mäntynen, M. Merimaa, F. Manoocheri, and E. Ikonen, "Use of the predictable quantum efficient detector with light sources of uncontrolled state of polarization," *Measurement Science and Technology*, accepted.

Author's contribution

The research presented in this thesis is mainly carried out at the Metrology Research Institute of Aalto University School of Electrical Engineering in close collaboration with the Centre for Metrology and Accreditation (MIKES). Some of the experiments have been performed at Czech Metrology Institute (CMI) and Physikalisch-Technische Bundesanstalt (PTB).

In Publication I the author carried out the calculations and prepared most of the manuscript.

In Publication II the author developed mathematical routines for the wedged-trap reflectance, carried out the modelling and prepared the manuscript.

For publication III the author provided the design parameter values of the photodiodes used to construct the Predictable Quantum Efficient Detector (PQED), contributed in defining the simulation result parameters, and estimated the reflectance loss term and the related uncertainty. The author contributed to the manuscript preparation.

In publication IV the author designed most of the custom made mechanics, contributed significantly in building and characterising the PQED detectors, prepared and carried out most of the experiments, analysed the results, modelled the reflectance and prepared most of the manuscript.

In Publication V the author had a large contribution in preparing the single photodiodes for characterization measurements and PQED detectors for the experiments with cryogenic radiometers. The author participated in part of the measurements at CMI and PTB. The author replaced one of the PQED photodiodes broken at PTB during a thunderstorm. The author contributed to the manuscript preparation.

In Publication VI the author developed most of the mathematical routines, carried out the modelling and prepared the manuscript.

List of abbreviations

CMI	Czech Metrology Institute, Czech Republic
MIKES	Centre for Metrology and Accreditation, Finland
NIST	National Institute of Standards and Technology, USA
NPL	National Physical Laboratory, UK
PTB	Physikalisch-Technische Bundesanstalt, Germany
CR	cryogenic radiometer
CVC	current-to-voltage converter
DVM	digital voltmeter
EQD	external quantum deficiency
EQE	external quantum efficiency
IQD	internal quantum deficiency
IQE	internal quantum efficiency
ppm	part per million
PQED	Predictable Quantum Efficient Detector
Si	Silicon
SiO_2	Silicon dioxide

List of symbols

c	speed of light in vacuum
e	elementary charge
$g(\lambda)$	quantum gain
h	Planck's constant
$i_{phot}(\lambda)$	spectrally dependent photocurrent
n	number of reflections inside trap detector
$P(\lambda)$	spectrally dependent optical power
$P_0(\lambda)$	optical power of incident light
$P_r(\lambda)$	optical power of reflected light
$R_m(\lambda)$	measured responsivity
$R_p(\lambda)$	predicted responsivity
$R_0(\lambda)$	ideal responsivity
$V(\lambda)$	Luminous sensitivity of human eye
β	angle between the photodiodes
$\delta(\lambda)$	spectrally dependent internal quantum deficiency
$\Delta_m(\lambda)$	measured external quantum efficiency
$\Delta_p(\lambda)$	predicted external quantum efficiency
λ	irradiation wavelength
ν	frequency of electromagnetic radiation
ρ	reflectance
$\rho(\lambda)$	spectral reflectance

1. Introduction

This thesis gives an overview of the development and analysis of the Predictable Quantum Efficient Detector (PQED) - a new high-accuracy optical radiometer based on custom made induced junction silicon photodiodes. The developed detector is meant to be used as a convenient primary standard to facilitate traceable measurements in radiometry and photometry, where the optical power and spectral responsivity are key quantities.

Radiometry and photometry describe and quantify optical radiation properties in a systematic manner by defining the associated quantities and units. After the redefinition of the unit of luminous intensity (candela) in 1979 [1] all the radiometric and photometric quantities in the International System of Units (SI - Le Système International d'Unités) describing light source properties are based on optical power expressed by the unit watt. For radiometric quantities this is simple to understand by the fact that the intensity of any electromagnetic radiation is expressed through the energy it carries. By the 1979 definition of the candela the photometric quantities became linked with their related radiometric quantities. This is done by defining the photometric base unit candela at a single frequency (corresponding to the wavelength of about 555 nm) and taking into account the responsivity of the average human eye using the luminous efficiency function $V(\lambda)$ at other wavelengths. In this way the definition of the candela means that the accuracy of any optical measurement quantified, by the associated SI unit, depends upon the accuracy of optical power measurement. For this reason the optical power (i.e. radiant flux) is considered as an essential quantity and the radiometry and photometry community continues to develop methods to improve the determination of radiant flux.

Radiant flux can be determined generally by two methods. Firstly, the source of the radiation is well characterized and the spectral properties of the emission can be determined through system parameters, or secondly the sensitivity of the light measuring detector is known and expressed through some measurable quantity. To ensure an unbroken chain of dissemination of the optical power scale, any radiometric source or detector needs to be calibrated against a standard traceable to a primary device. The

primary radiometric standard does not require calibration against any other radiometric standard and is thus considered to be absolute. The properties of an absolute optical power standard need to be such that the radiating or detecting properties of the device can be calculated purely by physical laws based on fundamental constants and/or parameters independent on the produced or detected radiation.

Absolute standards based on sources are such as black bodies [2-4] or synchrotron radiation sources [4-6]. There are also developments of single photon sources based on the correlated photon technique [7-8]. Such quantum based method of defining the absolute source is a fundamentally new approach in the field of source based radiometry and research on its applicability is still on-going [9].

Detector-based standards divide into thermal detectors such as electrical substitution radiometers and photon-to-electron converting detectors such as silicon photodiodes. The beginning of contemporary high accuracy optical radiation measurement era can be considered as the parallel development of the low-temperature electrical substitution radiometer – the absolute cryogenic radiometer [10] – and the self-calibration technique of silicon photodiodes whose responsivity was traceable to fundamental constants [11]. Both of these developments base on the idea of linking the optical power scale with the response of an absolute detector.

1.1   Absolute detector-based techniques of optical power measurements

1.1.1   Optical power scale based on quantum detectors

The most common quantum detectors used in optical radiometry are silicon based photodiodes. Before 1980's the silicon photodiodes have been mainly used as transfer standards traceable to black-body radiation or electrical substitution radiometer [12].These methods resulted at best with the relative uncertainty of 0.1 % and required substantial efforts to achieve such uncertainty level [13]. Typical calibration of a silicon photodetector yielded uncertainty of more than 1 % [14]. In 1979 Geist [15-16] proposed that the advanced knowledge of the physics of the silicon material will allow development of analytical models to predict the quantum efficiency of silicon photodiodes by linking the responsivity of the photodiode to fundamental constants and wavelength. Soon after that a self-calibration technique emerged showing that commercially available silicon based photodetectors can be used as absolute detectors with standard uncertainty as low as 0.05 % [11].

The photon energy conversion to a measurable amount of charge carriers is described by the internal quantum efficiency (IQE). The idea behind the self-calibration method is to measure the internal quantum deficiency (IQD) - defined as one minus IQE - by applying bias voltages so that the losses due to recombination of charge carriers are suppressed and the IQE will reach its saturation. The difference of the responsivities with and without the bias voltages is then a direct measure of IQD and it shows the deficiency from the ideal photon-to-electron conversion.

There are two main recombination regions in the conventional diffused pn-type silicon photodiodes for which different bias voltages have to be applied to reduce the recombination. The first is in the SiO_2/Si surface and the second is in deeper layers of the bulk after the depletion region [17]. To reduce the bulk recombination a reverse bias is applied which increases the depletion region from micrometer range to tens of micrometers and improves the charge carrier collection efficiency in the volume. The surface recombination due to minority carriers is reduced by applying oxide bias voltage via a transparent conductive layer of weak boric acid. It was assumed that after the removal of the thin solution layer the photodiode regains its conventional properties. The results of self-calibration technique were encouraging and some national metrology institutes realized their primary optical power scale based on this method [18]. Unfortunately it was discovered that the quantum efficiency of the photodiode decreased after applying the oxide bias technique making the self-calibration method less favourable for realizing silicon pn-type photodiodes as absolute detectors [19-20].

The problems of oxide bias measurements were somewhat alleviated with the usage of induced junction photodiodes by Zalewski and Duda [21]. Their prototype 4 - element detector showed 0.999 ± 0.002 quantum efficiency within wavelengths from 400 nm to 700 nm and was promoted as a 100 % quantum efficient detector. To achieve a uniformly high quantum efficiency throughout the given wavelengths, reverse bias voltages of 1.5 V to 50 V had to be applied. Longer wavelengths required higher bias voltages increasing to more than 100 V at 800 nm. Such high bias voltages introduced a problem of the increased dark current which sets limits to the lower end of usable power levels, especially at longer wavelengths. The shift towards induced junction photodiodes allowed abandoning the oxide bias technique but the need for reverse bias remained. Detectors based on Zalewski and Duda's original design were also commercialized and for some time they were an industry standard detector [22]. Nevertheless marketing problems stopped the availability of these devices and a competing technology based on cryogenic radiometry (CR) combined with trap

detectors, usually equipped with high quality Hamamatsu S1337-1010 photodiodes, diminished the need for these detectors. Trap detectors based on S1337 diodes are further discussed at the end of this section.

More recently a technique of hybrid self-calibration by Gran et al [23] has been developed. This method implements both purely relative measurements and a self-calibration technique. The method has shown to be capable realizing absolute scale based on silicon trap detectors within standard uncertainty of 0.04 %. The oxide bias method to determine the front region losses was replaced with relative measurements against spectrally flat pyroelectric detector. This measurement provides spectral shape of the detector which can be used to fit the front region losses. Similar approach is used to estimate the rear surface losses. The hybrid self-calibration method, however, involves four steps of measurements to characterize the detector and has not gained wider application in the radiometry community.

In all of the above cases the loss term associated with the reflectance was reduced by combining three or more photodiodes into a light trapping structure [21-22, 24-25]. An example of a three element reflection trap is shown in Figure 1.
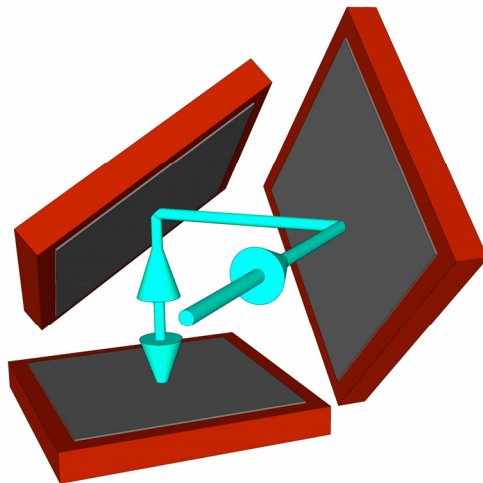
Figure 1. Trap detector consisting of three photodiodes. Five reflections and varying planes of incidence make this type of detector polarization independent.

The low reflectance of such device could be measured either at a single wavelength (laser based source) or derived from single photodiode reflectance measurements in the wavelength region of interest (usually monochromator based source). A more advanced approach to estimate the reflectance at extended range of wavelengths (UV-VIS-NIR) was to apply a physical model of thin film analysis [26-27]. This requires the knowledge of the layered structure of the used photodiodes and the associated material

parameters (indices of refraction). The structure of all silicon photodiodes is similar which allows analogous analytical approach if products of different manufactures are to be used. The method is to determine the thickness of the silicon dioxide which covers the bulk silicon and is the only thin film layer to be considered in the analysis. The model uses Fresnel equations and interfering multi-reflected beams within the oxide layer [28-29]. After measuring the reflectance at one or several laser wavelengths the oxide thickness could be determined and the reflectance at the rest of the wavelengths could be calculated relying on the oxide thickness gained by the model. This approach proved to be successful since model predictions were reliable and initial few measurements were easy to carry out.

In 1991 Fox introduced the concept of Hamamatsu S1337 silicon photodiode based transfer standard whose responsivity was highly predictable once calibrated against high accuracy primary standard only at a few discrete wavelengths [24]. Though S1337 based detectors are not absolute, they have quantum efficiency which is close to unity and their spectral responsivity is calculable throughout wavelengths of about 380 nm to 1000 nm. Such trap detectors, as they are called, are almost ideal transfer standards and their implementation in the optical power measurements has been of enormous importance. The successful development of the quantum efficiency model [30-32] combined with calculable reflectance losses allowed easy adoption of the trap detectors since the rest of the properties generally ascribed for an ideal relative spectral response standard were met: response over active area is uniform [33], linear [34-35] and stable with time [24]. Furthermore, the produced photocurrent has good signal-to-noise ratio and short time constant. All of this is obtained without applying a reverse bias voltage to the photodiodes. Those favourable properties have made possible to use trap detectors both as primary and secondary standards realizing both radiometric and photometric scales in many NMIs [36-41].

1.1.2 Optical power scale based on thermal detectors

High accuracy optical radiation measurement using thermal detectors started with the development and realization of the absolute cryogenic radiometer (CR) in 1980's at NPL [10, 42]. The original device was built for accurate estimation of the Stefan-Boltzmann constant [42], but with few modifications the device could be used also for precise optical radiation measurements. The principle of a cryogenic radiometer (Figure 2) is to measure the equivalent power of a radiation and an electric current. The

absorbing element in the radiometer is intermittently heated by the two sources. Both sources produce a thermal gradient in the absorbing cavity. The measurable power introduced by electric current can then be adjusted such that the temperature rise is equal to that of incident optical radiation. Based on heating current measurement the optical power can be determined. In practise the equality of the two heating methods is determined by electrical heating below and above the optical heating.

Low temperatures in the range of 4 K - 15 K are used to suppress the background radiation by shielding the cavity from room temperature; to prevent losses due to resistive heating of leads by using superconductive wires; to increase the thermal diffusivity of copper for uniform heat flux and for possibility to use large low reflectance cavity; to limit the thermal radiation of the cavity to minimum level, plus operating in vacuum eliminates the convective heat exchange [43].
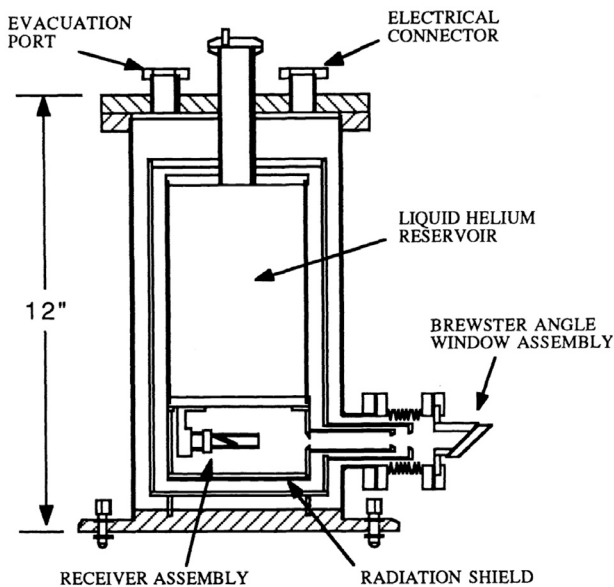
Figure 2. Example of a liquid helium cooled cryogenic radiometer. Figure from [44].

Typical CR allows optical radiation to be detected within relative standard uncertainty of 0.005 – 0.01 % [10, 31, 44-48] but the continued development of these devices has reduced the uncertainty below 0.003% [49, publication V]. Higher accuracies are achieved due to improved electrical power measurement, better control of the stray light and improved Brewster window transmittance estimation. The effect of Brewster window can be cancelled entirely using a joint Brewster window with the detector to be calibrated [publication V].

Conventionally the optical power scale of CR is transferred to secondary standards often realized by trap detectors as described in section 1.1.1. These trap detectors are usually equipped with commercially available high quality 10 x 10 mm² silicon photodiodes. The purpose is to deliver the high accuracy of CR at discrete wavelengths to a continuous wavelength range by the method of interpolation. First the trap detector is calibrated with CR at selected wavelengths and then its responsivity is extended to other wavelengths using similar analytical methods as originally used in self-calibration technique, i.e. the internal and external losses of the detector are calculated based upon physical models [30-32].

The calibration of trap detector transfer standards with CR increases the relative uncertainty to the typical value of 0.01 – 0.02 % [24, 46, 50]. There are many aspects in the increase of the uncertainty but one is related to the principal differences how these devices are functioning. CR is spectrally flat, i.e. it measures the power of the radiation irrelevant of the wavelength. Photodiodes on the other hand convert photons to charge carriers. The measured photocurrent depends on the radiation power and also on the wavelength. To perform high accuracy calibration of trap detector against CR requires that the irradiation wavelength is precisely known. This is only achievable with fully monochromatic narrow bandwidth laser lines. Another criterion for reliable scale transfer is the stability of the light source. Laser beams can be stabilized to the order of ten ppm over half an hour [publication V], but monochromator based sources do not reach such low stability. Monitor detector correction is not sufficient here due to the large time constant of CR [49]. Also the effect of stray light is dissimilar for detectors with spectral responsivities of different shape. All of these aspects would be alleviated if the primary and secondary standards would be both based on solid state detectors.

The process of calibration requires a sophisticated control mechanism to operate the CR and trap detector in a combined manner as shown in Figure 3. Majority of the components are involved in the control mechanism of the CR.

Though the CR has some advantages - e.g. spectral flatness and wide wavelength range – its operation is expensive and initial investment into equipment is rather large. Handling of this equipment requires qualified personnel familiar with the specific CR. Additionally, CR based measurements are time consuming due to long preparation time required to cool down the cavity either by using liquid nitrogen and liquid helium or by applying mechanical cooling. Another disadvantage of the CR is its poor transportability. Usually the CR, vacuum pumps, cooling equipment and dedicated electronics occupy large amount of laboratory space.
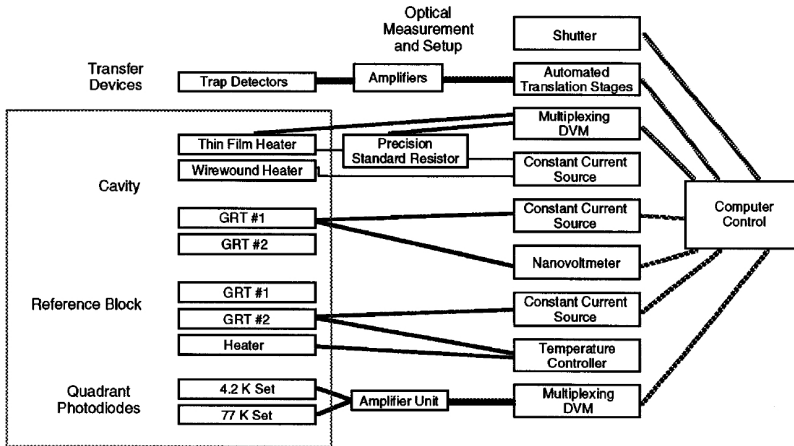
Figure 3. Example diagram of the CR measurement instrumentation used in NIST. The elements surrounded by the box are inside the CR Dewar. Most of the controlling apparatus is required for operating the CR. Such complex instrumentation is typical for all CR systems. See also Figure 14 showing the simple instrumentation setup if the primary standard is realized with a solid state detector. Figure taken from [47]

There are clear needs for simpler calibration methods either to transfer the optical power scale to photodiode-based secondary standards which are portable and easily configurable into various measurement setups or develop a primary standard which itself is comparable with the operability of transfer standards. This ambition has again raised interest towards the original development of absolute detectors based on induced junction photodiodes. The objective of this work is concentrated on the new advancements of the induced junction photodiodes and to study the applicability of a quantum detector based on such photodiodes as a primary standard of optical power.

1.2 Progress of the work

After the proposal of using the custom made induced junction photodiodes in precise measurements of optical radiation [51], it became evident that the optical losses in the planned detector have to be considerably smaller than in contemporary trap detectors. A reduction from 3000 ppm (parts per million) to below 100 ppm was required. First an analysis was carried out to estimate what are the lowest theoretical levels of specular reflectance that can be achieved using only a single large area photodiode (publication I). Calculations showed that at Brewster angle the reflectances can be reduced down to 90 ppm to 2 ppm on selected visible wavelengths of p-polarized light. This method required a thick oxide layer

of the order of 3 μm on top of silicon to act as antireflection coating on multiple wavelengths. A hemispherical mirror was proposed to cover the photodiode to control the diffused part of the reflectance.

A more efficient way to reduce specular reflectance at all visible wavelengths was proposed in publication II. The low level of reflectance was achieved using photodiodes in a wedge-like trap structure so that multiple reflections take place before the light escapes the detector. The assembly of the photodiodes so that they face each other had the advantage of collecting also the small fraction of scattered light though it was found that the diffuse reflectance from such photodiodes is a minor effect. Analytical estimation showed that photodiodes with oxide-thicknesses of around 100 nm will be the best to achieve the lowest reflectances. Such a thin oxide thickness was favoured compared to the μm range outcome of the single photodiode calculation due to the fact that growing a thermal oxide is a time consuming process.

The advanced modelling of internal quantum deficiency (IQD) of the produced PQED photodiodes in publication III predicted that as low as 1 ppm charge carrier losses are achievable at liquid nitrogen temperatures at shorter than 600 nm wavelengths of visible light and below 100 ppm at wavelengths between 600 nm and 720 nm. The predictions were also promising at room temperature where the uncertainties of internal losses of photodiodes were estimated to be below 90 ppm over all visible wavelengths.

Publication IV describes the structure of the induced junction photodiodes, covers the design of the prototype PQED and estimates the predicted responsivity at liquid nitrogen and at room temperature. The estimated responsivity includes the measurements and calculations of the reflectance losses combined with the predictions of internal losses of publication III and gives thorough uncertainty analysis for the results.

The prototype PQED was compared with the present primary standard of optical power - the cryogenic radiometer – at two laboratories at the wavelengths of 476 nm, 532 nm and 760 nm. The results are reported in publication V showing the agreement of measured values with the predicted results within the expanded standard uncertainty at 95 % confidence level. This article addresses also the non-linearity and spatial uniformity of responsivity of individual induced junction photodiodes showing that they are highly linear and that their spatial uniformity is comparable with the high quality commercially available silicon photodiodes.

Usually the PQED is operated in a sealed chamber, such as a cryostat, and the transmission of the light into the chamber is achieved using p-polarized collimated beam through a Brewster-angled window. Publication VI

analyses the reflectance losses and related uncertainty of the room temperature PQED without a window under the illumination of varied polarization of light. The outcome was that a simple photocurrent ratio measurement of individual PQED photodiodes predicts the effects of polarization through which the reflectance can be estimated. This allows light sources with any polarization to be used and still maintain similar low uncertainty that was previously available only for p-polarized light.

2. Predictable Quantum Efficient Detector

The responsivity of any quantum detector can be expressed using elementary charge (e), Planck's constant (h), speed of light in vacuum (c), and the vacuum wavelength λ. If the detector would be ideal no losses would occur and the listed constants would describe entirely the ideal responsivity $R_0(\lambda) = e\lambda/hc$ of a photodetector. This comes from the principle that each absorbed photon produces exactly one charge carrier in the detector. Photon carries an energy of $h\nu = hc/\lambda$. If photon is absorbed it adds an elementary charge e to the electric current. The energy carried per unit time by the photons is described by the optical power whereas the amount of charge carriers per unit time is expressed by the produced photocurrent. The responsivity of a quantum detector is thus given in units of amperes per watt.

In reality no detector is perfect and losses take place. These losses can be divided as reflectance losses and charge carrier losses or external losses and internal losses. Equation (1) describes the responsivity of a real photodetector,

$$R_p(\lambda) = \frac{e\lambda}{hc} \left[1 - \rho(\lambda)\right]\left[1 - \delta(\lambda)\right]\left[1 + g(\lambda)\right]. \tag{1}$$

The loss/gain corrections in square brackets are reflectance $- \rho(\lambda)$, charge carrier losses $- \delta(\lambda)$, and quantum gain $- g(\lambda)$. The quantum gain describes a rare situation where the built-in voltage in the photodiode accelerates charge carriers and due to impact ionization secondary carriers are produced. It is many of orders of magnitude weaker contribution than the loss corrections and thus it is often neglected in calculations [51, publication III]. As seen from equation (1) the responsivity of a photodetector can approach the responsivity of an ideal quantum detector if the loss corrections are minimized to zero. This raises the question if the losses in advanced quantum detectors can be reduced sufficiently so that the optical powers measured with such detectors can approach or even surpass the accuracy of the present primary standard. In the following this is discussed in more detail showing that remarkably low level losses can be

obtained using custom made induced junction photodiodes so that the uncertainty of the responsivity is of the same order of magnitude as the absolute values of the loss corrections and are comparable with the uncertainty of a cryogenic radiometer.

2.1 Induced junction photodiodes and charge carrier losses

Induced junction photodiodes are high efficiency silicon-based photodetectors where the presence of natural surface charge in silicon dioxide is used to generate the electric field inside the bulk silicon [52]. These photodiodes have many advantages as compared to the regular diffused junction photodiodes to suppress the charge carrier losses.

Sufficiently thick oxide layer holds enough positive charge to produce an n-type inversion layer and therefore also to generate a depletion region close to the SiO_2/Si boundary in low-doped p-type silicon (Figure 4). Low doping concentration of the order of 10^{12} - 10^{13} cm^{-3} has a major role of suppressing the bulk recombination losses and is required to balance the charge distribution for proper generation of the depletion region. The closeness of the depletion region to the SiO_2/Si boundary helps to avoid surface recombination, which is a significant loss term in regular diffused pn - junction photodiodes at short visible wavelengths. To extend the depletion region deeper into the substrate, around tens of micrometers [17, publication III], a reverse bias voltage of 5 V to 20 V is applied. This helps to collect charge carriers generated by the lower energy photons of the visible range.
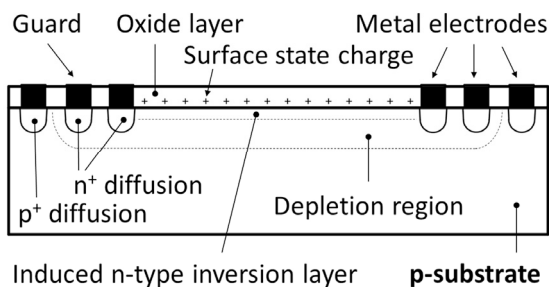

Figure 4. Simplified cross-section of the developed induced junction photodiodes (not to scale). For reflectance loss calculations, also a nanometer range mixture layer of SiO_2 and Si at the oxide - silicon interface and a top layer of ice-like water on SiO_2 are used, but not depicted here. (Publication IV).

The efficiency of the surface charge generation in the oxide depends on the processing methods and oxide growing temperatures but also on the thickness of the SiO_2 layer [52, 53]. Reportedly oxides thicker than 70 nm should produce enough surface charge so that the inversion condition is fulfilled and the processed silicon chip works as a photodiode [21, 52]. We

found that at the used doping concentrations this condition was not true and oxides thicker than 100 nm have to be used. The exact selection of oxide thicknesses is discussed in the next section as this affects also the reflectance properties of the detector.

An additional option to improve the charge carrier collection is to lower the temperature of the photodiode. At low temperatures the charge carrier transport is affected less by lattice vibrations allowing photon-generated electrons and holes to move inside the semiconductor with reduced losses. Preliminary modelling by Geist et al [51] showed that the temperature of liquid nitrogen is sufficient to suppress the charge carrier transport losses to the level of 1 ppm. The temperature of 77 K is considerably easier to reach than the 4 K – 15 K range where the cryogenic radiometers are operated.

Thorough modelling of the internal quantum deficiency was carried out with PC1D solar cell software [54]. Similar software was used in the original Geist et al work in 2003. Since the PC1D approach is one dimensional, a more sophisticated 3D Synopsys Sentaurus[1] was used to compare the results of the two software packages. It was found that PC1D predicts three to ten times lower losses than the 3D software [publication III]. This is most probably caused by the fact that the charge carriers have to move a long distance along the SiO_2/Si interface outside the illuminated volume before being collected by the electrode. The PC1D software cannot estimate those charge carrier losses. Comparison of two software packages led to the conclusion that simple one dimensional approach to predict the IQD of an induced junction photodiode is sufficient, but for reliable uncertainty estimation the results of PC1D have to be multiplied by ten. Figure 5 depicts the predicted IQD at room temperature and at 77 K showing that at low temperature internal losses and their uncertainties smaller than 1 ppm can be obtained at wavelengths from 400 nm to 600 nm. At longer wavelengths the absorption coefficient of silicon decreases so that the charge carrier generation happens beyond the depletion region. This explains the fast increase of IQD in red and near-IR wavelengths. At room temperature, where the absorption coefficient is four to nine times larger at shown wavelengths, the wavelength dependence of the absorption coefficient allows almost constant IQD at all visible wavelengths.

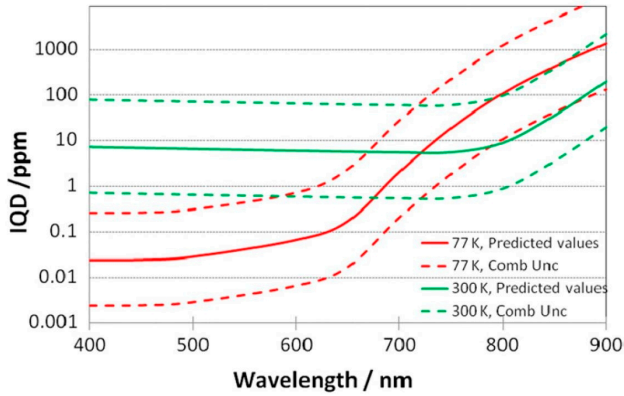[1] Access to Synopsys Sentarus software was limited during the work.

Figure 5. Predicted internal quantum deficiency (IQD) of an induced junction photodiode at the temperatures of 300 K and 77 K with reverse bias voltage of 5 V. The dashed lines show standard uncertainty mainly caused by the reliability of the PC1D software. (Publication III).

2.2 Reflectance losses

2.2.1 Specular reflectance

The specular reflectance of a silicon based photodiode is in the order of 30 % [29] at normal incidence. One method to reduce the reflectance below 100 ppm or even 1 ppm, i.e. to the level similar of the predicted IQD, is to use a wedged trap configuration so that incident light will reflect multiple times between the two photodiodes (Figure 6) before escaping the detector [22, 55-57, publication II].

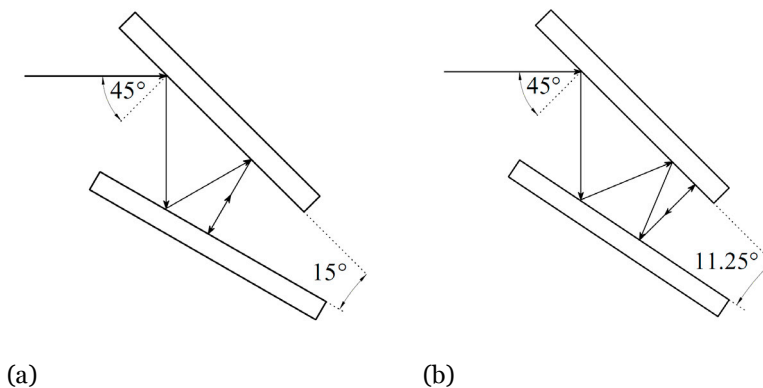(a)   (b)

Figure 6. Wedged trap structure reducing specular reflectance: (a) using 7 reflections and (b) using 9 reflections between the photodiodes.

Figure 6 shows the beam path inside 7 - and 9 - reflection trap detectors, indicating also the angle between the photodiodes. The angle β between the photodiodes is calculable using the following equation

$$\beta = \frac{45°}{(n-1)/2} \ , \qquad\qquad (2)$$

where n denotes the number of reflections.

In the alignment process sufficiently high laser power can be used so that the back reflection becomes observable. For that purpose it is beneficial to have the reflected beam to nominally follow a similar path as the incident beam. By adjusting the incoming and outgoing beams close to each other the PQED can be aligned properly in the measurement system. Correct positioning of the PQED assures that reflectance losses are similar and predictable when repeating the experiments.

It is desired to have the reflectance of the detector as small as possible with minimum number of reflections. High number of reflections increases the required size of the active area which will have an impact on the cost of the photodiodes. A more favourable approach is to tailor the oxide thickness on top of silicon so that it behaves as an antireflection coating. Further reduction in reflectance can be made if p - polarized light is used. This condition is usually met since the light polarized in the plane of incidence is required also for high accuracy measurements with cryogenic radiometers.

Calculations show that favourably low level of reflectance is achieved over all visible wavelengths when oxide thicknesses of around 300 nm and 220 nm are used for the upper and lower photodiode, respectively (see Figure 6). Figure 7 shows the reflectances of such 7 - and 9 - reflection traps in several orientations of polarization plane indicating significantly lower reflectance at p - polarized light.

(a)　　　　　　　　　　　　　　　　　　(b)
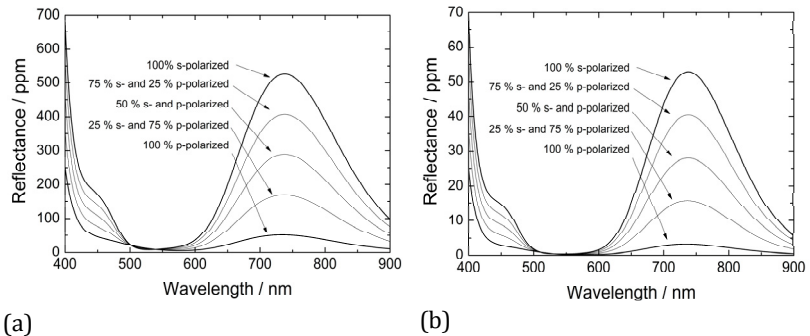
Figure 7. Reflectance of (a) 7-reflection and (b) 9-reflection PQED showing the dependence on the polarization of the incident beam. Using seven reflections and p-polarized light, reflectance below 60 ppm can be achieved over most of the visible wavelengths. Nine reflections will further decrease the reflectance by a factor of about 10. (Publication VI).

Publications II, IV and VI give a thorough overview of the reflectance properties of the wedged-style trap, estimating also the uncertainties

caused by the material parameters and construction tolerances of the trap [publications IV, VI].

2.2.2   Diffuse reflectance

Reflectance of a surface is defined as the ratio of the reflected optical power (or flux) $P_r(\lambda)$ relative to the incoming optical power $P_0(\lambda)$ as given in equation 3,

$$\rho(\lambda) = \frac{P_r(\lambda)}{P_0(\lambda)}. \tag{3}$$

Reflected power $P_r(\lambda)$ contains both specular and diffuse parts of the reflected flux. The models of specular reflectance for silicon photodiodes have been proven to predict the total reflectance losses with an uncertainty of $2 \cdot 10^{-3}$ [29] using Fresnel equations. That accuracy has been sufficient to predict reflectance losses of transfer standards meaning that the magnitude of the diffuse component is sufficiently small compared to the specular component so that most of the time it can be neglected in the reflectance loss term of the trap detectors based on silicon photodiodes.

As shown in the previous section, the IQD of induced junction photodiodes is argued to be predictable with an uncertainty below 1 ppm. The multireflection trap of Figure 6b can reduce the specular part of the reflectance to similarly low level. Such small value of reflectance requires also accurate estimation of the diffuse component. This can be reliably done using an experimental approach described in section 2.4.4. Even if the diffuse reflectance of a single photodiode is larger than 1 ppm, the design of the wedge trap structure where the photodiodes face towards each other and cover a large solid angle will help to reduce the effect of diffuse reflectance losses to sub ppm level.

2.3   Predicted responsivity

Equation (1) in the beginning of section 2 describes the responsivity of a quantum detector. There the combination of factors $[1 - \rho(\lambda)]$ and $[1 - \delta(\lambda)]$ describes the external quantum efficiency (EQE) of the detector, where $\rho(\lambda)$ is the reflectance loss and $\delta(\lambda)$ is the internal quantum deficiency. Since $\rho(\lambda)$ and $\delta(\lambda)$ are sufficiently small the EQE can be written as $1 - \rho(\lambda) - \delta(\lambda)$. It is convenient to use the term external quantum deficiency (one minus EQE) to estimate the efficiency of the incident photon-to-electron conversion. Then the net effect of loss terms $\rho(\lambda) + \delta(\lambda)$ describes the fractional part of the photons which do not produce charge carriers in the

measurement circuit. This is also the basis for the predicted responsivity, which is related to EQD as

$$\Delta_p(\lambda) = 1 - \frac{R_p(\lambda)}{R_0(\lambda)} = \rho(\lambda) + \delta(\lambda),$$ (4)

where $\Delta_p(\lambda)$ is the predicted external quantum deficiency, $R_p(\lambda)$ is the predicted responsivity of the PQED and $R_0(\lambda)$ is the responsivity of an ideal photodetector.

The uncertainty of the predicted responsivity depends on the uncertainty of the wavelength and the uncertainties of the components of the EQD, i.e. the reflectance and IQD. For a stabilized monochromatic light source the wavelength can be determined with an accuracy better than 1 ppm [58]. The uncertainties due to calculated reflectance and IQD are determined by the accuracies of the physical models and the uncertainties of the material parameters used in these models [publications III, IV]. The uncertainty of the calculated reflectance can be further reduced by directly measuring the reflectance using a rather conventional measurement setup [publication IV]. An uncertainty of 1 % in reflectance of 100 ppm would still be sufficient to determine the relative uncertainty of the responsivity within ~1 ppm.

2.4 Prototype PQED and characterization

2.4.1 PQED photodiodes and detector structure

The custom-made induced junction photodiodes were produced using lightly p‑doped <111> oriented silicon wafers with thickness of 525 μm. The measured doping concentration of boron was about 2×10^{12} cm^{-3}. The photodiode active area is surrounded by three metal contact rings (Figure 8). The photocurrent is registered via the innermost and outermost contacts through which also the bias voltage is applied. The intermediate 'guard' is used, when necessary, to suppress the noise due to surface leakage, which may be relatively large in p-type materials as compared with n-type materials. The guard ring is then connected to the common ground which is also the ground potential of the bias voltage.

The prototype PQED was realized using the 7-reflection trap configuration in order to facilitate the alignment and use the advantage of slightly higher reflectance during reflectance loss measurements as compared with the 9-reflection trap. Higher reflectance was not considered as a drawback since it can be estimated with an uncertainty close to the predicted charge carrier losses.
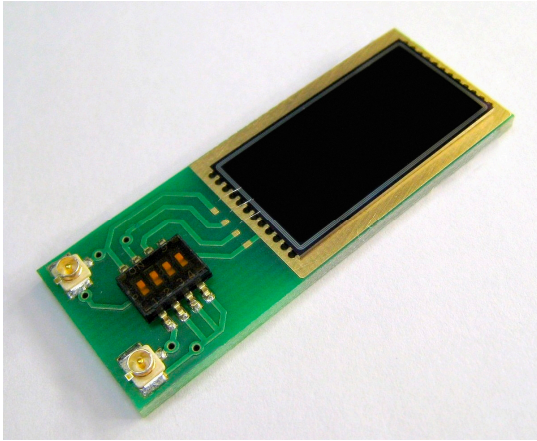
Figure 8. Processed PQED photodiode mounted on the PCB board. Photocurrent is registered using the U.FL connectors. Same contacts are used to apply the bias voltage. The small 4-channel switch routes signals between contacts and allows using different operational modes, when necessary. (Publication IV).

2.4.2 PQED photodiode uniformity

The uniformities of spatial responsivity of the PQED photodiodes were measured using a computer controlled x-y translator [59, publication V]. To maintain the clean environment and to be able to carry out measurements also at low temperatures, the individual photodiodes were installed into a liquid nitrogen cryostat. The Brewster window and the cryostat were attached to each other using a flexible bellows. This enabled the movement of the cryostat without changing the position of the window to cancel the effect of the non-uniformity of the Brewster window.

The measurements were carried out at the wavelength of 760 nm by moving the laser spot row by row in 0.5 mm steps across the photodiode surface. A reference measurement at the central area of the photodiode was used to normalize the photocurrents for each row to correct any other effect than the fluctuations in the laser power. The stability of the laser intensity was monitored and later corrected using a trap detector.

The uniformity of the spatial responsivity is described as a standard deviation relative to the central area for the photodiode. For the photodiode with 220 nm oxide thickness it was around 0.045 % whereas for the 300 nm oxide photodiode it was around 0.060 %. The results given here are for 10 V reverse bias to maximise the effect of the internal quantum efficiency though results at lower reverse bias voltage of 5 V were very similar [publication V]. The reported spatial uniformities are comparable with uniformities of high quality commercially available photodiodes such as Hamamatsu S1337 [60, 61].
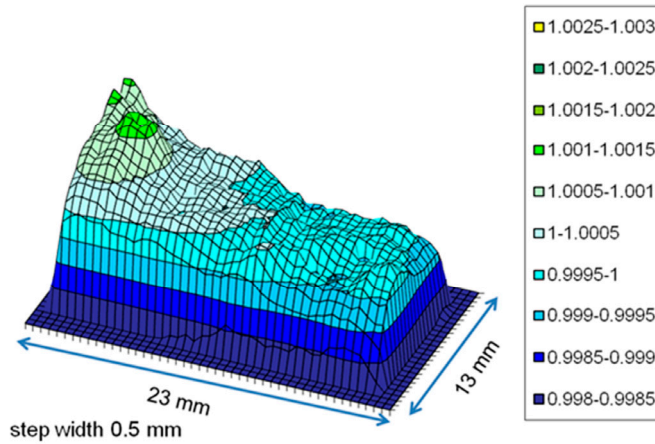
Figure 9. Example of the relative uniformity of responsivity of the PQED photodiode with the oxide thickness of 220 nm. Scanning was done at room temperature with laser wavelength of 760 nm. Figure from [59].

Figure 9 shows an example of the spatial uniformity of the photodiode with an oxide thickness of 220 nm indicating a slope-like structure in the spatial responsivity. Smooth change in responsivity is explainable with the possible slope in the oxide thickness expected to be present in thermally grown oxides. A variation of about 0.8 nm in the oxide thickness corresponds to a change in the relative responsivity of 0.25 % shown in Figure 9 in the inner part of the photodiode. Similar variations in the oxide thickness have been measured with ellipsometric technique [61]. This shows that the spatial non-uniformity of responsivity is strongly related to the non-uniformity in the oxide thickness and indicates the high spatial uniformity of charge carrier generation within the PQED photodiode.

A change of 1 nm in oxide thickness affects the responsivity of the 7-reflection PQED by less than 3 ppm over most of the visible wavelengths increasing to about 10 ppm at short visible wavelengths around 400 nm.

2.4.3   PQED photodiode non-linearity

The linearity of the PQED photodiodes was measured with a setup described in [62] with modifications to adapt the stabilized DFB laser (760 nm) into the measurement system. Measurements showed no significant non-linearity within the standard uncertainty of 30 ppm up to photocurrents of 160 μA (~250 μW at 760 nm). Figure 10 shows the results of the linearity measurement of the PQED photodiode with an oxide thickness of 300 nm. The non-linearity of a photodiode with an oxide thickness of 220 nm showed similar behaviour.
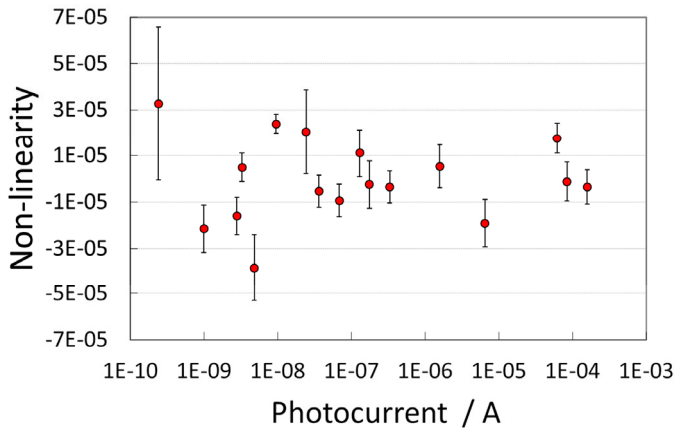
Figure 10. Non-linearity of a single PQED photodiode with oxide thickness of 300 nm. The measurements were performed at the room temperature with reverse bias voltage of 5 V. Photocurrents were measured up to currents of 160 μA (~250 μW) at the irradiation wavelength of 760 nm. Within standard uncertainty of 3×10^{-5} no non-linearity was detected.

A photodiode with an oxide thickness of 220 nm was also measured at higher power levels up to 1 mW. It was discovered that the photodiode becomes noticeably nonlinear at photocurrents of ~400 μA (approximately 600 μW at 760 nm). In the PQED the photocurrent is distributed between two photodiodes, but single photodiode non-linearity measurements are highly relevant for this case, because (80 ± 10) % of the photocurrent is produced by the first photodiode. A thorough analysis of the PQED photodiode spatial uniformity characterization and non-linearity measurements is given in publication V.

2.4.4 PQED measured specular and diffuse reflectance

Specular reflectance of an assembled PQED was measured at the wavelengths of 476 nm, 488 nm and 532 nm. Comparing the measured results with the modelled values indicates a few ppm smaller values as expected. Figure 11 shows the graph of the predicted reflectance with standard uncertainty estimation and the measured reflectances at selected wavelengths.
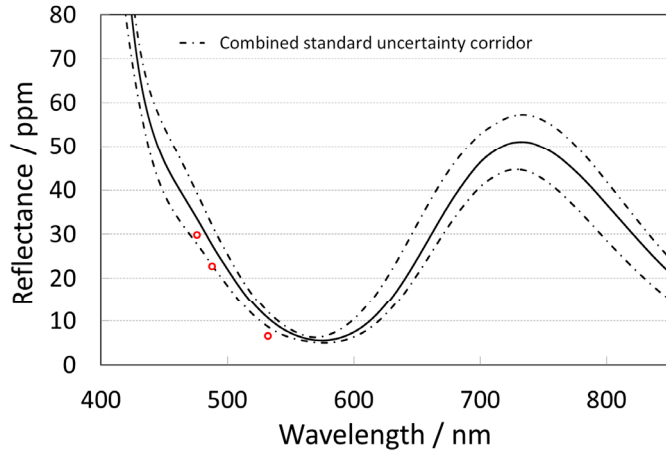
Figure 11. Measured (dots) and calculated (continuous line) reflectance of the 7-reflection PQED at room temperature. The uncertainties of measurements are smaller than the dot sizes. Dashed lines indicate the standard uncertainty of calculations due the material parameters, alignment and geometrical tolerances. (Publication IV).

The values of the measured reflectances are 29.8 ± 0.2, 22.8 ± 0.4 and 6.62 ± 0.05 ppm at the vacuum wavelengths of 476.4 nm, 488.1 and 532.3 nm, respectively. The corresponding modelled values are 33.4 ± 12.5, 27.5 ± 9.2 and 10.7 ± 4.0 ppm, respectively. The uncertainties are given at the 95 % confidence level. The measured reflectances are determined with significantly lower uncertainty and thus these values at the corresponding wavelengths were used in the calculations of the predicted IQD.

The effect of the probable ice growth on top of the photodiodes at low temperature due to evaporating water from the cryostat walls was estimated at the temperature of 77 K by long term measurements over 60 h at the wavelengths of 488 nm and 532 nm. The ice growth is difficult to avoid using vacuum systems with lowest pressures of 10^{-6} mbar [63] and especially when the chamber is repeatedly exposed to laboratory air due to the development phase of the photodetector. The cryostats housing the PQED detectors were also non-bakeable prohibiting reduction of the amount of the trapped water molecules inside the vacuum chamber.

Oscillating patterns of PQED reflectance agree with measurement reports where water vapour at low temperatures is intentionally introduced into the vacuum chamber [64-66]. These reports also claim that the growing ice is highly transparent and uniform without producing significant scattering at liquid nitrogen temperatures.

The variation of reflectance at low temperatures increased the standard uncertainty of the predicted quantum efficiency by about 5– 8 ppm except at short wavelengths around 400 nm where the standard uncertainty increased to 50 ppm (publication IV).

The diffuse part of the reflected light at room temperature was estimated by measuring the scattering from a processed silicon wafer which was only exposed to a clean room environment [67]. The equipment used in this measurement is routinely used for silicon wafer scattering measurements at the collaborating company Okmetic Oyj. The measurements revealed low level of scattering of the order of 0.05 ppm on the photodiode active areas and slightly increased scattering of 0.5 ppm on the implanted electrodes. These values demonstrate highly clean surfaces of PQED photodiodes and indicate that the diffuse component in reflectance is sufficiently small.

Publication IV gives in depth characterization of the PQED reflectance. The results obtained therein were used to estimate the responsivity and internal quantum efficiency of the PQED.

2.4.5   PQED measured responsivity

The responsivity of the PQED was measured using two different cryogenic radiometer systems, one at PTB [publication V] and one at CMI [48, publication V]. At PTB the advantageous structure of a joint Brewster window for CR and PQED helped to reduce the uncertainty due to the losses when the propagating beam goes through the window. At CMI a more conventional method was used where the CR and PQED were compared by interchanging the detectors in front of the beam. Both the CR and PQED had their own Brewster windows in the CMI experiments. The wavelengths used at PTB measurements were 532 nm and 760 nm, whereas at CMI only 476 nm was used. A more detailed description of measurement systems and the related uncertainties are given in publication V, where tables 2 and 3 list the major uncertainty components of the two CR measurement systems used to validate the predicted responsivity of PQED.

External quantum deficiency of the PQED is validated by comparing the predicted EQD (see equation 4) with the measured EQD $\Delta_m(\lambda)$ as described by equation (5),

$$\Delta_m(\lambda) = 1 - \frac{R_m(\lambda)}{R_0(\lambda)}. \tag{5}$$

The measured responsivity $R_m(\lambda)$ is obtained by the equation

$$R_m(\lambda) = \frac{i_{phot}(\lambda)}{P(\lambda)}, \tag{6}$$

where $i_{phot}(\lambda)$ is the photocurrent measured with the PQED and $P(\lambda)$ is the optical power of the same beam measured by the cryogenic radiometer.

Figure 12 shows the schematic of the PTB system where the PQED and CR are intermittently aligned into the laser beam using a computer controlled arc-shaped rail.
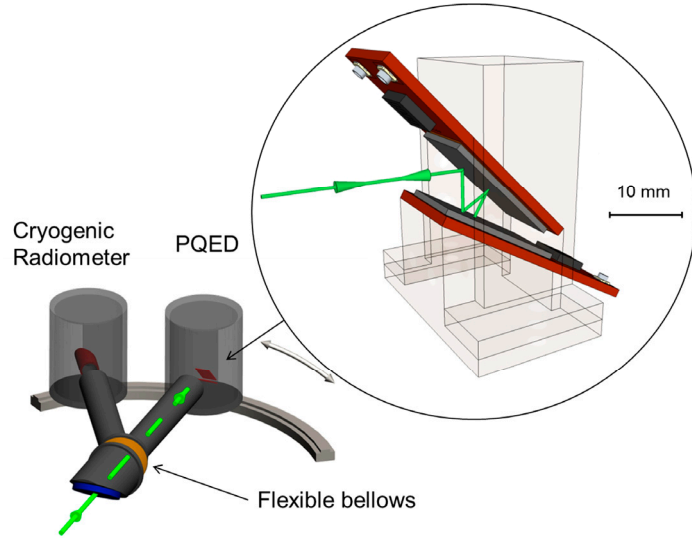

Figure 12. PQED responsivity measurement setup at PTB showing the cryogenic radiometer and PQED on an arc-shaped rail behind the joint Brewster window. The magnified section of PQED shows the photodiode arrangement inside a copper holder (semi-transparent area) for efficient heat transfer from the cryostat cold finger to the photodiodes.

The measurements were carried out at room temperature and at liquid nitrogen temperature. First the responsivity dependence on reverse bias voltage was determined to adjust the bias voltage so that the PQED would operate in saturated internal quantum efficiency regime. The photocurrent dependence on the bias voltage was measured at the wavelengths of 532 nm and 760 nm at room temperature and at liquid nitrogen temperature. At 532 nm saturation occurred at reverse bias voltages greater than 1 V at both 298 K and 77 K, however at 760 nm this condition was only met at 298 K whereas a reverse bias greater than 20 V was required at 77 K. This result is in agreement with the modelled IQD indicating sudden increase of charge carrier losses above the wavelength of 650 nm. The reason is the reduced absorption coefficient of silicon at low temperatures [68, 69] which causes the photons at longer wavelengths to be absorbed beyond the depletion region deep in the bulk. At room temperature the bias voltage of -5V is sufficient for saturated quantum efficiency operation at all wavelengths in the covered range of 400 nm to 800 nm.

The comparison of the measured and predicted external quantum deficiency of the PQED is shown in Figure 13. The predicted loss described by the solid line is the sum of the predicted reflectance $\rho(\lambda)$ and the predicted internal quantum deficiency $\delta(\lambda)$. At room temperature the shape

of the predicted EQD is affected mostly by the spectral reflectance whereas its uncertainty is high due to the uncertainty of the predicted IQD. At low temperature the shape and uncertainty of the predicted EQD from 400 nm to 750 nm are affected by the reflectance. The predicted IQD at this wavelength range is below 1 ppm.
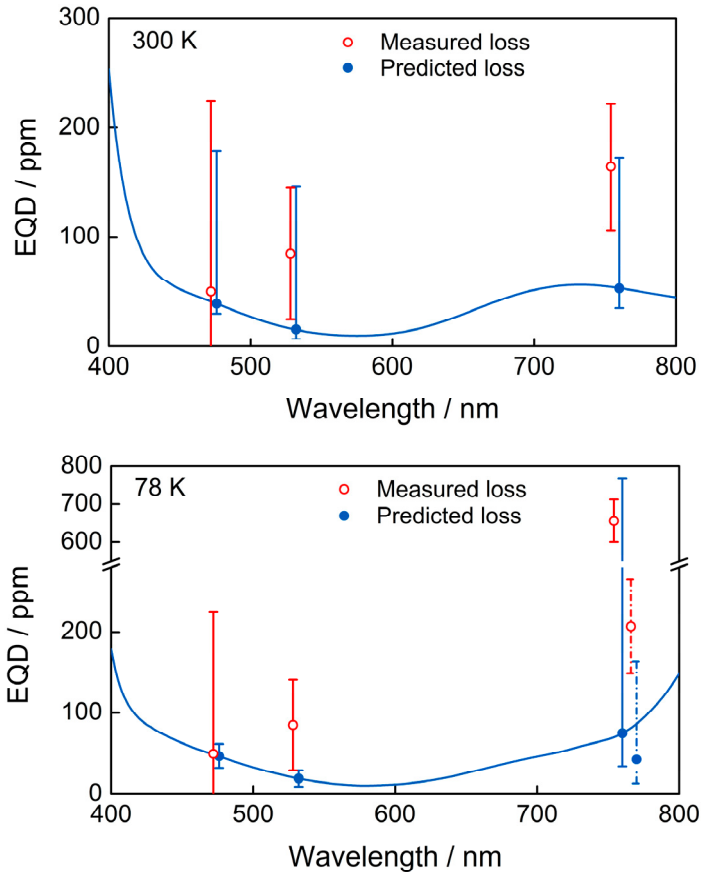

Figure 13. Measured and predicted external quantum deficiency (EQD) at room temperature and at liquid nitrogen temperature with reverse bias voltage of 5V. Measurements were made at the wavelengths of 476 nm, 532 nm and 760 nm. The uncertainty bars show expanded uncertainty in the confidence level of 95 %. The points with dashed uncertainty bars indicate predicted and measured EQD and their uncertainties at the reverse bias voltage of 20V.

At longer wavelengths above 750 nm the predicted EQD is mostly affected by the increased IQD (see Figure 5) due to reduced absorption coefficient of silicon. The high uncertainty at these wavelengths is caused by the combination of the reliability of PC1D modelling and the uncertainty of the absorption coefficient of silicon (see publication IV).

Results in Figure 13 indicate agreement of the predicted responsivity with the measured responsivity within the uncertainties. Though there seems to be systematic underestimation of the predicted quantum deficiency the measurements show typically below 100 ppm EQD with similar order of

magnitude uncertainty. Somewhat unexpected results are obtained at low temperatures where the measured EQD is in the same level with the EQD at room temperature. This on the other hand indicates that an improved modelling of the IQD with reduced uncertainty is required since that is by far the largest component in the uncertainty of the room temperature EQD [publications III, IV]. Internal quantum deficiency at the room temperature is estimated to be below 180 ppm (k = 2) due to recombination losses with a nominal value of about 10 ppm whereas at low temperature a value below 1 ppm is expected. In spite of that the results at room temperature are comparable with the accuracy of a typical commercial grade CR. This gives promising indications that calibrations with cryogenic radiometers at visible wavelengths may be replaceable with PQED devices operated at room temperature.

2.5 Operability of PQED

The measurement system containing the PQED and a conventional trap detector at room temperature is comparable with the simple setup of comparing two trap detectors. A typical measurement scheme is shown in Figure 14 indicating that only a fraction of the devices is required as compared to the complicated system needed for CR measurements (see Figure 3). For photocurrent registration a high accuracy current detection system is utilized usually consisting of a low noise current-to-voltage converter (with biasing option for PQED) and digital voltmeter. For precise alignment and switching of detectors automated translators are used. All of these devices can be controlled with a computer driven system enabling full automation of the measurement process.
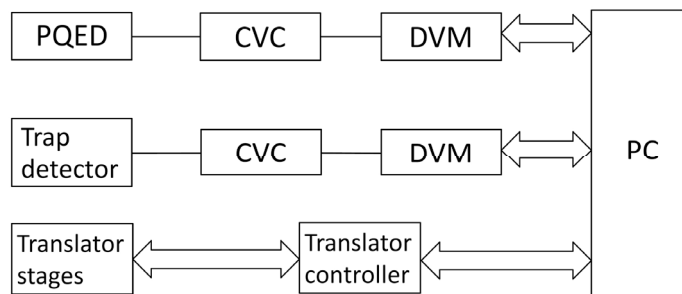

Figure 14. Simple measurement setup transferring the optical power scale from PQED to trap detectors. CVC – current-to-voltage converter, DVM – digital voltmeter, PC – computer control of the devices.

3. Conclusions and outlook

A novel photodetector – the Predictable Quantum Efficient Detector (PQED) – has been designed, constructed and characterised. The PQED consists of custom made lightly doped induced junction silicon photodiodes, which significantly reduce the charge carrier losses mainly caused by the bulk and surface recombination. Two such photodiodes are arranged in a wedged trap structure to reduce the reflectance losses to similarly low levels as the internal losses.

Predictions suggest that with optimal conditions the photon-to-electron conversion is achievable with losses below 1 ppm with similar low uncertainty at a wide range of visible wavelengths. This requires the detector operation at liquid nitrogen temperature and within clean environment preventing any surface contamination of the photodiodes. The prototype PQED has been designed to closely follow the required operational conditions to achieve as low uncertainty in the photon-to-electron conversion process as possible. At low temperature the lowest external quantum deficiency (EQD) was predicted to be 20 ppm with 10 ppm expanded uncertainty. At room temperature, where the operation of the PQED is considerably easier, the EQD at the wavelength range from 450 nm to 800 nm was predicted to be below 60 ppm, although with large uncertainty up to 180 ppm. At shorter wavelengths from 400 nm to 450 nm the predicted EQE was as high as 260 ppm, but this was caused by the increase in reflectance, whose expanded uncertainty was typically below 70 ppm. Only at wavelengths below 410 nm the expanded uncertainty increased above 100 ppm peaking at 400 nm with the value of 140 ppm. Thus the predicted EQD in room temperature had rather uniform uncertainty of 120 ppm to 180 ppm ($k = 2$) throughout all visible wavelengths caused by EQE whereas the variation in EQE was caused mainly by the reflectance.

Validation of the PQED has been performed by comparing the detector against the present primary standard of optical power - the cryogenic radiometer (CR). The lowest expanded uncertainty achieved by the validation measurements was 56 ppm. Within that uncertainty the predicted and measured EQD of the PQED overlapped showing that available models predicting internal quantum deficiency have become

reliable and sufficiently accurate. These results are comparable with the accuracy of CR, especially when a joint window of the CR and the calibrated detector is not used, indicating that calibrations with cryogenic radiometers at visible wavelengths may be replaceable with PQED devices operated at room temperature. Developments towards this approach are actively carried out. A compact room temperature PQED is already in prototyping phase.

There are many improvements to be made to enhance the predictability of the PQED both at low temperature and at room temperature. For this study only one-dimensional software PC1D was mostly available. A versatile three-dimensional software would especially improve the reliability of the room temperature responsivity values. An improved vacuum system would reduce the effects causing the time dependence of the reflectance at low temperature. At long visible wavelengths, where uncertainty of the IQD at low temperature is large, the improved determination of silicon extinction coefficient would reduce the uncertainty of the predicted responsivity.

Stability of the PQED is a property to be tested. Regular silicon photodiodes show drift in responsivity at short visible wavelengths around 400 nm [70, 71]. However the induced junction photodiodes have much smaller impurity concentration which is believed to be the cause of instability in diffused photodiodes. For that reason the instability has not been considered to be significant in PQED detector though further research has to be carried out.

4. References

[1]   *Comptes rendus de la 16ᵉ CGPM* (1979)

[2]   Blevin W R and Steiner B "Redefinition of the Candela and the Lumen"
        Metrologia **11** 97–104 (1975)

[3]   Sapritsky V I "Black-body radiometry" *Metrologia* **32** 411–7 (1995)

[4]   Hollandt J, Seidel J, Klein R, Ulm G, Migdall A and Ware M "Primary
        sources for use in radiometry" *Optical Radiometry* ed A Parr, J Gardner and
        R Datla (Amsterdam: Elsevier, Academic) pp 213–90 (2005)

[5]   Ulm G "Radiometry with synchrotron radiation" *Metrologia* **40** S101–S106
        (2003)

[6]   Klein R, Brandt G, Fliegauf R, Hoehl A, Müller R, Thornagel R, Ulm G,
        Abo-Bakr M, Feikes J, Hartrott M, Holldack K and Wüstefeld G "Operation
        of the Metrology Light Source as a primary radiation source standard"
        Physical Review Special Topics - Accelerators and Beams **11** 1–10 (2008)

[7]   Klyshko D N "*Photons and Nonlinear Optics*" (New York: Gordon and
        Breach) (1988)

[8]   Migdall A "Differences Explained in Correlated-Photon Metrology
        Techniques" *Physics Today* **52** 15 (1999)

[9]   Cheung J Y, Chunnilall C J, Woolliams E R, Fox N P, Mountford J R,
        Wang J and Thomas P J "The quantum candela: a re-definition of the
        standard units for optical radiation" *Journal of Modern Optics* **54** 373–96
        (2007)

[10]   Martin J E, Fox N P and Key P J "A cryogenic radiometer for absolute
        radiometric measurements" *Metrologia* **21** 147–55 (1985)

[11]   Zalewski E F and Geist J "Silicon photodiode absolute spectral response
        self-calibration" *Applied Optics* **19** 1214–6 (1980)

[12]   Hengstberger F "The absolute measurement of radiant power" *Absolute
        Radiometry* ed F Hengstberger (London: Academic Press) pp 1–117 (1989)

[13]   Blevin W R and Brown W J "A Precise Measurement of the Stefan-
        Boltzmann Constant" *Metrologia* **7** 15–29 (1971)

[14]   Geist J, Steiner B, Schaefer R, Zalewski E and Corrons A "Electrically
        based spectral power measurements through use of a tunable cw laser"
        Applied Physics Letters **26** 309 (1975)

[15] Geist J "Quantum efficiency of the p-n junction in silicon as an absolute radiometric standard." *Applied optics* **18** 760–2 (1979)

[16] Geist J "On the possibility of an absolute radiometric standard based on the quantum efficiency of a silicon photodiode" *Proc. SPIE, Measurements of Optical Radiations* vol 196 ed H P Field, E F Zalewski and F M Zweibaum pp 75–83 (1979)

[17] Geist J, Zalewski E and Schaefer A "Spectral response self-calibration and interpolation of silicon photodiodes" *Applied Optics* **19** 3795–9 (1980)

[18] Geist J "Current Status Of, And Future Directions In, Silicon Photodiode Self-Calibration" *Proc. SPIE*, *Optical Radiation Measurements II* vol 119 ed J M Palmer pp 246–56 (1989)

[19] Verdebout J and Booker R L "Degradation of native oxide passivated silicon photodiodes by repeated oxide bias" *Journal of Applied Physics* **55** 406–12 (1984)

[20] Key P J, Fox N P and Rastello M L "Oxide-bias Measurements in the Silicon Photodiode Self-calibration Technique" *Metrologia* **21** 81–7 (1985)

[21] Zalewski E F and Duda C R "Silicon photodiode device with 100% external quantum efficiency" *Applied optics* **22** 2867–73 (1983)

[22] Palmer J M "Alternative Configurations for Trap Detectors" *Metrologia* **30** 327–33 (1993)

[23] Gran J "*Accurate and independent spectral response scale based on silicon trap detectors and spectrally invariant detectors*" Dissertation for the degree of Doctor Scientiarum, (University of Oslo) (2005)

[24] Fox N "Trap detectors and their properties" *Metrologia* **28** 197–202 (1991)

[25] Bittar A "Extension of a silicon-based detector spectral responsivity scale into the ultraviolet" *Metrologia* **32 (6)**, 407 – 500 (1996)

[26] Huen T "Reflectance of thinly oxidized silicon at normal incidence." *Applied optics* **18** 1927–32 (1979)

[27] Saito T, Katori K and Onuki H "Characteristics of semiconductor photodiodes in the VUV region" *Physica Scripta* **41** 783–7 (1990)

[28] Born M and Wolf E "*Principles of Optics*" (Oxford: Pergamon) (1965)

[29] Haapalinna A, Kärhä P and Ikonen E "Spectral reflectance of silicon photodiodes" *Applied optics* **37** 729–32 (1998)

[30] Gentile T R, Houston J M and Cromer C L "Realization of a scale of absolute spectral response using the National Institute of Standards and Technology high-accuracy cryogenic radiometer" *Applied Optics* **35** 4392–4403 (1996)

[31]   Werner L, Fischer J, Johannsen U and Hartmann J "Accurate determination of the spectral responsivity of silicon trap detectors between 238 nm and 1015 nm using a laser-based cryogenic radiometer" *Metrologia* **37** 279–84 (2000)

[32]   Kübarsepp T, Kärhä P and Ikonen E "Interpolation of the spectral responsivity of silicon photodetectors in the near ultraviolet" *Applied optics* **39** 9–15 (2000)

[33]   White M G and Bittar A "Uniformity of Quantum Efficiency of Single and Trap-configured Silicon Photodiodes" *Metrologia* **30** 361–4 (1993)

[34]   Fischer J and Fu L "Photodiode nonlinearity measurement with an intensity stabilized laser as a radiation source" *Applied Optics* **32** 4187–90 (1993)

[35]   Kübarsepp T, Haapalinna a, Kärhä P and Ikonen E "Nonlinearity measurements of silicon photodetectors." *Applied optics* **37** 2716–22 (1998)

[36]   Kärhä P "*Trap Detectors and Their Applications in the Realization of Spectral Responsivity, Luminous Intensity and Spectral Irradiance Scales*" Thesis for the degree of Doctor of Technology (Helsinki University of Technology) (1997)

[37]   Kübarsepp T "*Optical radiometry using silicon photodetectors*" Thesis for the degree of Doctor of Technology (Helsinki University of Technology) (1999)

[38]   Hartree W S, Fox N P and Lambe R P "Towards a detector-based spectral-radiance scale in the near-ultraviolet" *Metrologia* **32** 519–22 (1995)

[39]   Larason T, Bruce S and Cromer C "The NIST high accuracy scale for absolute spectral response from 406 nm to 920 nm" *Journal of research - National Institute of Standards and Technology* **101** 133–40 (1996)

[40]   Bittar A, Hamlin J D, White M G "*A New Detector Based Spectral Responsivity Scale for the 400 nm to 900 nm Wavelength Range*" Industrial Research Limited Report 91, Lower Hutt, New Zealand (1993)

[41]   Bazkir O and Samadov F "Characterization of silicon photodiode-based trap detectors and establishment of spectral responsivity scale" *Optics and Lasers in Engineering* **43** 131–41 (2005)

[42]   Quinn T J and Martin J E "A Radiometric Determination of the Stefan-Boltzmann Constant and Thermodynamic Temperatures between -40 degrees C and +100 degrees C" *Philosophical Transactions of the Royal Society A: Mathematical, Physical and Engineering Sciences* **316** 85–189 (1985)

[43]   Fox N "Radiometry with cryogenic radiometers and semiconductor photodiodes" *Metrologia* **96** 535–43 (1995)

[44]   Hoyt C C, Miller P J, Foukal P V. and Zalewski E F "Comparison Between A Side-Viewing Cryogenic Radiometer And Self-Calibrated Silicon Photodiodes" *Proc. SPIE, Optical Radiation Measurements II* vol 1109 ed J M Palmer pp 236–45 (1989)

[45] Varpula T, Seppa H and Saari J-M "Optical power calibrator based on a stabilized green He-Ne laser and a cryogenic absolute radiometer" *IEEE Transactions on Instrumentation and Measurement* **38** 558–64 (1989)

[46] Nield K M, Clare J F, Hamlin J D and Bittar A "Calibration of a trap detector against a cryogenic radiometer" *Metrologia* **35** 581–6 (1998)

[47] Gentile T R, Parr A C, Houston J M, Hardis J E and Cromer C L "National Institute of Standards and Technology high-accuracy cryogenic radiometer" *Applied Optics* **35** 1056 – 68(1996)

[48] Fox N P, Haycocks P R, Martin J E and Ul-Haq I "A mechanically cooled portable cryogenic radiometer" *Metrologia* **32** 581–4 (1995)

[49] Stock K D, Hofer H, White M and Fox N P "Lowest uncertainty direct comparison of a mechanically-cooled and a helium-cooled cryogenic radiometer" *Metrologia* **37** 437–9 (2000)

[50] Fox N P and Martin J E "Comparison of two cryogenic radiometers by determining the absolute spectral responsivity of silicon photodiodes with an uncertainty of 0.02%." *Applied optics* **29** 4686–93 (1990)

[51] Geist J, Brida G and Rastello M L "Prospects for improving the accuracy of silicon photodiode self-calibration with custom cryogenic photodiodes" *Metrologia* **40** S132–S135 (2003)

[52] Hansen T "Silicon UV-photodiodes using natural inversion layers" *Physica Scripta* **18** 471–5 (1978)

[53] Hoem S, Gran J, Sildoja M, Manoocheri F, Ikonen E and Müller I "Physics of self-induced photodiodes" *Proc. of NEWRAD 2011 Conference* ed S Park and E Ikonen (Hawaii, USA) pp 259–60 (2011)

[54] Clugston D A and Basore P A "PC1D version 5: 32-bit solar cell modelling on personal computers" *Proc. 26th IEEE Photovoltaic Specialists Conference* (Anaheim, CA) pp 207–10 (1997)

[55] Lehman J H "Pyroelectric Trap Detector for Spectral Responsivity Measurements" *Applied Optics* **36** 9117–8 (1997)

[56] Lehman J, Sauvageau J, Vayshenker I, Cromer C and Foley K "Silicon wedge-trap detector for optical fibre power measurements" *Measurement Science and Technology* **9** 1694–8 (1998)

[57] Canfield L R, Vest R E, Korde R, Schmidtke H and Desor R "Absolute silicon photodiodes for 160 nm to 254 nm photons" *Metrologia* **35** 329–34 (1998)

[58] Quinn T J "Practical realization of the definition of the metre, including recommended radiations of other optical frequency standards (2001)" *Metrologia* **40** 103–33 (2003)

[59]   Müller I, Brida G, Gran J, Hoem S, Ikonen E, Kübarsepp T, Linke U, Manoocheri F, Sildoja M, Smid M, Socaciu-Siebert L and Werner L "Predictable Quantum Efficient Detector II: Characterization Results" *Proc of NEWRAD 2011 Conference* ed S Park and E Ikonen (Hawaii, USA) pp 209–10 (2011)

[60]   Bittar A and White M G "High-resolution spatial uniformity of surface reflectance and response of silicon photodiodes" Proc. SPIE, 14th Symposium on photonic measurements vol 1712, ed J Schanda and T Lippenyi pp 121–31 (1993)

[61]   White M, Lolli L, Brida G, Gran J and Rajteri M "Optical constants and spatial uniformity of thermally grown oxide layer of custom, induced-junction, silicon photodiodes for a predictable quantum efficient detector" *Journal of Applied Physics* **113** 243509 (2013)

[62]   Lei F and Fischer J "Characterization of Photodiodes in the UV and Visible Spectral Region Based on Cryogenic Radiometry" *Metrologia* **30** 297–303 (1993)

[63]   Berman A "Water vapor in vacuum systems" *Vacuum* **47** 327–32 (1996)

[64]   Brown D E, George S M, Huang C, Wong E K L, Rider K B, Smith R S and Kay B D "H 2 O Condensation Coefficient and Refractive Index for Vapor-Deposited Ice from Molecular Beam and Optical Interference Measurements" *The Journal of Physical Chemistry* **100** 4988–95 (1996)

[65]   Westley M S, Baratta G A and Baragiola R A "Density and index of refraction of water ice films vapor deposited at low temperatures" *The Journal of Chemical Physics* **108** 3321–6 (1998)

[66]   Berland B S, Brown D E, Tolbert M A and George S M "Refractive index and density of vapor-deposited ice" *Geophysical Research Letters* **22** 3493–6 (1995)

[67]   Ikonen E, Haapalinna A, Sildoja M and Manoocheri F "Photon-to-electron converter with 1 ppm quantum deficiency" *Proc. of Northern Otpics 2009 Conf.* (Vilnius, Lithuania) p 114 (2009)

[68]   Dash W and Newman R "Intrinsic Optical Absorption in Single-Crystal Germanium and Silicon at 77°K and 300°K" *Physical Review* **99** 1151–5 (1955)

[69]   Green M A "Self-consistent optical parameters of intrinsic silicon at 300K including temperature coefficients" *Solar Energy Materials and Solar Cells* **92** 1305–10 (2008)

[70]   Werner L "Ultraviolet stability of silicon photodiodes" *Metrologia* **35** 407–11 (1998)

[71]   Goebel R and Stock M "Report on the comparison CCPR-K2.b of spectral responsivity measurements in the range 300 nm to 1000 nm" *Metrologia* **41** 02004–89 (2004)

BUSINESS +
ECONOMY

ART +
DESIGN +
ARCHITECTURE

SCIENCE +
TECHNOLOGY

CROSSOVER

DOCTORAL
DISSERTATIONS